International Journal of Mechanical and Materials Engineering (IJMME), Vol.5 (2010), No.2, 251-259

COMPUTATIONAL SIMULATION ON EMISSIONS OF HYDROGEN FUELED COMPRESSION IGNITION ENGINE WITH VARIABLE COMBUSTION TEMPERATURE

R. Adnan[a], H.H. Masjuki[b] and T.M.I. Mahlia[b,c]
[a] Department of Mechanical Engineering, University Tenaga Nasional, Kajang, Selangor, Malaysia
[b] Department of Mechanical Engineering, University of Malaya, 50603 Kuala Lumpur, Malaysia
[c] Department of Mechanical Engineering, Syiah Kuala University, Banda Aceh 23111, Indonesia
Email: adnanr@uniten.edu.my

Received 13 October 2010, Accepted 19 October 2010

ABSTRACT

In this paper, computational simulation on the effect of combustion temperature on emissions characteristics of hydrogen-fuelled compression ignition engine was performed. Combustion process was modeled based on Equilibrium Constant Method (ECM) and programmed using MATLAB program in order to calculate mole fractions of 18 combustion products when hydrogen-diesel fuels blends is burnt at variable combustion temperatures. It is observed that throughout all equivalence ratios, higher temperature increases H_2, CO, HCN, atoms C, O and H, NO, OH, NO_2 and O_3 emissions and decreases CO_2, H_2O, NH3 and CH_4, N_2, O_2 and HNO_3 emissions. The highest H_2O emission occurs during stoichiometric combustion and decrease in combustion temperature causes insignificant changes in atom N emission.

***Keywords*:** Equilibrium Constants Method; Newton-Raphson Iteration; MATLAB; Combustion Model; Emission Characteristics

1. INTRODUCTION

The use of alternative fuel in diesel engines has received more attention for over the past two decades. The unavailability of petroleum-based fuel has created a need to seek for the possible use of alternative fuels.
Hydrogen has found vast applications in fields such as aerospace, electricity generation and internal combustion engines. Hydrogen fuel cell provides electrical power in the space program to the shuttle and its by-product of water is consumed by the crew (Brenda, 2005). In the field of combustion engine, the use of hydrogen fuel either directly or indirectly is not new. Experiments have been done decades before to investigate the effectiveness of using hydrogen as a fuel. Hydrogen offers a possible solution to such problems as energy security resource availability, and environmental concerns. Many researchers have used hydrogen as a fuel in spark ignition (SI) engine. Caton (2001) reported a significant reduction in power output, pre-ignition, backfire and knocking problems at high load were observed when inducing hydrogen in SI engine within a limited operation range. Saravanan et al (2008) concluded that hydrogen fuel cannot be used as a sole fuel in a diesel engine due to lower compression temperature in order to initiate the combustion since hydrogen has higher self-ignition temperature. Hence, diesel fuel is used as an ignition source for hydrogen-diesel fuels blends combustion engine. Xing-hua et al (2008) reported the simplest method of using hydrogen in a diesel engine is to run in the dual fuel mode with diesel as the main fuel that can act as an ignition source for hydrogen. In a hydrogen-diesel dual fuel engine, the main fuel is either inducted/carbureted or injected into the intake air stream with combustion initiated by the diesel. The major energy is obtained from diesel while the rest of the energy is supplied by hydrogen.

Most research in hydrogen-diesel fuelled compression ignition engine has concentrated on experimental study of performance and emission. Karim, et al (2003) concluded that at low loads, much of the primary gaseous fuel remain unburned leading to high hydrocarbon (HC) and CO emissions. At high loads a large amount of gaseous fuel admission results in uncontrolled reaction rates near the pilot spray causing rough engine operation. Perini et al. (2010) developed the two zone quasi-dimensional model to simulate the combustion process in SI engines fueled with hydrogen, methane or hydrogen-methane blends. Roy et al. (2009) investigated the effect of hydrogen addition in the producer gas on the performance and emissions of a supercharged dual fuel diesel engine fueled at constant injection pressure and hydrogen quantity. Ma et al. (2003) have developed computer simulation to predict the performance of a hydrogen fueled engines. The mathematical models to predict pressure, net heat release rate, mean gas temperature, and brake thermal efficiency for dual fuel diesel engine operated on hydrogen, LPG and mixture of LPG and hydrogen as secondary fuels were developed by Lata et al (2010). Verhelst et al (2007) have developed a quasi-dimensional two-zone combustion model framework to calculate the pressure and temperature in hydrogen engines. Wang et al (2010) have developed a multidimensional model based on CFD and coupled with detail reaction kinetics to study the combustion process in H_2/CNG engine. Computer simulation of hydrogen combustion was conducted by Masood et al

(2008) using Low Temperature Combustion Model Method (LTCM) with only 10 product species, concluded significant reduction in CO_2 and NO_x.

In this present study, combustion model of hydrogen-diesel dual fuel blends was developed to study the effect of its combustion temperature on emissions. Based on Equilibrium Constant Method (ECM), a computer program using MATLAB has been developed for the blended fuels to calculate mole fractions of emissions.

2. COMBUSTION MODELING APPROACH

This section presents a solution for the properties of equilibrium combustion products based on an equilibrium constant method applied to the gas phase products of combustion of fuels. Equilibrium constant is based on thermodynamic measurements and empirical calculations; it is very accurate and precise in solving most of chemical kinetics problems by recognizing that, at equilibrium, the forward and reverse reaction rates must be equal (Stephen, 2000). Thermodynamic data for combustion products and many other pollutants are available in a compilation published by the National Bureau of Standards, called the JANAF (Joint Army–Navy–Air Force) tables (1971). The equilibrium constant data from JANAF tables using polynomial curve fitted had been used in calculating the combustion products (Stull, 1971). In this study, the derivations of governing equations for the reaction combustion equation need to be emphasized. 18 product species were assumed in this study and a system of 19-nonlinear equations appear from derivation of the reaction combustion equation. The 19-nonlinear system of equations can be solved using Newton-Raphson methods prior to its implementation into MATLAB program.

2.1. Governing Equations

Combustion of hydrocarbon fuels at low temperature produces N_2, H_2O, CO_2 and O_2 in lean mixtures ($\phi<1$) and N_2, H_2O, CO_2, CO and H_2 in rich mixtures ($\phi>1$). At higher temperatures (usually above 1600K), these major species dissociate and react to form additional species with significant amounts (Ganesan, 2003). By considering dissociation process of major product species in combustion, then the reaction combustion equation for any hydrocarbon and hydrogen mixture fuels with air can be written as:

$$n_f C_\alpha H_\beta + pH_2 + \frac{a_s}{\phi}(O_2 + 3.76N_2) \longrightarrow n_T[y_1H_2 + y_2H_2O + y_3CO_2 + y_4N_2 + y_5O + y_6O_2 + y_7O_3 + y_8H + y_9OH + y_{10}CO + y_{11}C + y_{12}CH_4 + y_{13}NO + y_{14}NO_2 + y_{15}NH_3 + y_{16}HNO_3 + y_{17}HCN + y_{18}N] \quad \text{--(1)}$$

For diesel fuel used in this simulation program, the subscripts α and β are given as 14.4 and 24.9, respectively. The stoichiometric molar air-fuel ratio,

$$a_s = \left[n_f\alpha + \left(\frac{n_f\beta + 2p}{4} \right) \right] \quad \text{--- (2)}$$

From concentration conditions at equilibrium, the summation of the mole fraction of each product species equals unity, then:

$$y_1 + y_2 + y_3 + y_4 + y_5 + y_6 + y_7 + y_8 + y_9 + y_{10} + y_{11} + y_{12} + y_{13} + y_{14} + y_{15} + y_{16} + y_{17} + y_{18} = 1 \quad \text{--- (3)}$$

In combustion modeling, it is necessary to calculate the equilibrium constant, K, from a polynomial equation. Therefore, the equilibrium constant values were taken from JANAF Tables and fitted by Agrawal et al (1977) with the following general form:

For temperature range of 1600K to 4000K:

$$\begin{aligned} Log_{10}K_i = {} & A_1 + A_2(T-1600)(10^{-3}) + A_3(T-1600)(T-2000)(10^{-6}) \\ & + A_4(T-1600)(T-2000)(T-2400)(10^{-9}) \\ & + A_5(T-1600)(T-2000)(T-2400)(T-2800)(10^{-12}) \\ & + A_6(T-1600)(T-2000)(T-2400)(T-2800)(T-3200)(10^{-15}) \\ & + A_7(T-1600)(T-2000)(T-2400)(T-2800)(T-3200) \\ & (T-3600)(10^{-18}) \end{aligned} \quad \text{--- (4)}$$

For temperature range of 4000K to 6000K:

$$\begin{aligned} Log_{10}K_i = {} & A_8 + A_9(T-4000)(10^{-3}) + A_{10}(T-4000)(T-4500)(10^{-6}) \\ & + A_{11}(T-4000)(T-4500)(T-5000)(10^{-9}) \\ & + A_{12}(T-4000)(T-4500)(T-5000)(T-5500)(10^{-12}) \end{aligned} \quad \text{--- (5)}$$

From the balance of atoms on both sides in Equation (1), the following four equations can be obtained:

$$n_T(y_3 + y_{10} + y_{11} + y_{12} + y_{17}) = n_f\alpha \quad \text{--- (6a)}$$

$$n_T(2y_1 + 2y_2 + y_8 + y_9 + 4y_{12} + 3y_{15} + y_{16} + y_{17}) = n_f\beta + 2p \quad \text{--- (6b)}$$

$$n_T(y_2 + 2y_3 + y_5 + 2y_6 + 3y_7 + y_9 + y_{10} + y_{13} + 2y_{14} + 3y_{16}) = \frac{2a_s}{\phi} \quad \text{--- (6c)}$$

$$n_T(2y_4 + y_{13} + y_{14} + y_{15} + y_{16} + y_{17} + y_{18}) = \frac{7.52a_s}{\phi} \quad \text{--- (6d)}$$

From chemical equilibrium equations, fourteen equations of the equilibrium constants that relate the mole fractions of combustion products were used in describing these problems and shown as below:

$$K_1 = \left(\frac{y_{10}y_6^{0.5}}{y_3} \right)(P)^{0.5}; \quad K_2 = \left(\frac{y_{11}y_6^{0.5}}{y_{10}} \right)(P)^{0.5};$$

$$K_3 = \left(\frac{y_{11}y_1^2}{y_{12}} \right)(P)^2; \quad K_4 = \left(\frac{y_{11}y_1^{0.5}y_4^{0.5}}{y_{17}} \right)(P);$$

$$K_5 = \left(\frac{y_1y_6^{0.5}}{y_2} \right)(P)^{0.5}; \quad K_6 = \left(\frac{y_9y_1^{0.5}}{y_2} \right)(P)^{0.5};$$

$$K_7 = \left(\frac{y_8}{y_1^{0.5}} \right)(P)^{0.5}; \quad K_8 = \left(\frac{y_5}{y_6^{0.5}} \right)(P)^{0.5};$$

$$K_9=\left(\frac{y_7}{y_6^{1.5}}\right)(P)^{-0.5}\ ;\ K_{10}=\left(\frac{y_{18}}{y_4^{0.5}}\right)(P)^{0.5}\ ;$$

$$K_{11}=\left(\frac{y_{13}}{y_4^{0.5}y_6^{0.5}}\right)(P)^{0}\ ;\ K_{12}=\left(\frac{y_{13}y_6^{0.5}}{y_{14}}\right)(P)^{0.5};$$

$$K_{13}=\left(\frac{y_4^{0.5}y_1^{1.5}}{y_{15}}\right)(P)\ \text{and}\ K_{14}=\left(\frac{y_{14}^3y_2}{y_{13}y_{16}^2}\right)(P).$$

--- (7)

The expression for the equilibrium constants can be rearranged to express mole fractions of all the species in terms of y_i where i = 1,2,3,….,18 which represents mole fraction of each species as written in Eq.(1).

$$y_5=c_5c_8\left(\frac{y_2}{y_1}\right);\quad y_6=c_5^2\left(\frac{y_2^2}{y_1^2}\right)\ ;\ y_7=c_5^3c_9\left(\frac{y_2^3}{y_1^3}\right);$$

$$y_8=c_7y_1^{0.5}\ ;\ y_9=c_6\left(\frac{y_2}{y_1^{0.5}}\right);\ y_{10}=\left(\frac{c_1}{c_5}\right)\left(\frac{y_1y_3}{y_2}\right);$$

$$y_{11}=\left(\frac{c_1c_2}{c_5^2}\right)\left(\frac{y_1^2y_3}{y_2^2}\right);\ y_{12}=\left(\frac{c_1c_2c_3}{c_5^2}\right)\left(\frac{y_1^4y_3}{y_2^2}\right);$$

$$y_{13}=c_5c_{11}\left(\frac{y_2y_4^{0.5}}{y_1}\right)\ ;\ y_{14}=c_5^2c_{11}c_{12}\left(\frac{y_2^2y_4^{0.5}}{y_1^2}\right);$$

$$y_{15}=c_{13}y_4^{0.5}y_1^{1.5};\ y_{16}=c_5^{2.5}c_{11}c_{12}^{1.5}c_{14}^{0.5}\left(\frac{y_2^3y_4^{0.5}}{y_1^{2.5}}\right);$$

$$y_{17}=\left(\frac{c_1c_2c_4}{c_5^2}\right)\left(\frac{y_1^{2.5}y_3y_4^{0.5}}{y_2^2}\right)\ \text{and}\ \ y_{18}=c_{10}y_4^{0.5}$$

--- (8)

Where:

$$c_1=\frac{K_1}{P^{0.5}}\ ;\ c_2=\frac{K_2}{P^{0.5}}\ ;\ c_3=\frac{P^2}{K_3}\ ;\ c_4=\frac{P}{K_4}\ ;\ c_5=\frac{K_5}{P^{0.5}}\ ;$$

$$c_6=\frac{K_6}{P^{0.5}}\ ;\ c_7=\frac{K_7}{P^{0.5}};\ c_8=\frac{K_8}{P^{0.5}}\ c_9=K_9P^{0.5};$$

$$c_{10}=\frac{K_{10}}{P^{0.5}};\ c_{11}=K_{11}\ ;\ c_{12}=\frac{P^{0.5}}{K_{12}}\ ;\ c_{13}=\frac{P}{K_{13}}\quad\text{and}$$

$$c_{14}=\frac{P}{K_{14}}$$

--- (9)

The total number of mole, n_T can be eliminated by dividing Equation (6b) with Equation (6a) and yields:

$$2y_1+2y_2-\left(\frac{n_f\beta+2p}{n_f\alpha}\right)y_3+y_8+y_9-\left(\frac{n_f\beta+2p}{n_f\alpha}\right)y_{10}-\left(\frac{n_f\beta+2p}{n_f\alpha}\right)y_{11}$$
$$+\left[4-\left(\frac{n_f\beta+2p}{n_f\alpha}\right)\right]y_{12}+3y_{15}+y_{16}+\left[1-\left(\frac{n_f\beta+2p}{n_f\alpha}\right)\right]y_{17}=0$$

--- (10)

Likewise Equations (6c) and (6d) can be divided with the Equation (6a), respectively to obtain:

$$y_2+\left[2-\left(\frac{2a_s}{n_f\alpha\phi}\right)\right]y_3+y_5+2y_6+3y_7+y_9+\left[1-\left(\frac{2a_s}{n_f\alpha\phi}\right)\right]y_{10}-\left(\frac{2a_s}{n_f\alpha\phi}\right)y_{11}$$
$$-\left(\frac{2a_s}{n_f\alpha\phi}\right)y_{12}+y_{13}+2y_{14}+3y_{16}-\left(\frac{2a_s}{n_f\alpha\phi}\right)y_{17}=0$$

--- (11)

and

$$-\left(\frac{7.52a_s}{n_f\alpha\phi}\right)y_3+2y_4-\left(\frac{7.52a_s}{n_f\alpha\phi}\right)y_{10}-\left(\frac{7.52a_s}{n_f\alpha\phi}\right)y_{11}-\left(\frac{7.52a_s}{n_f\alpha\phi}\right)y_{12}$$
$$+y_{13}+y_{14}+y_{15}+y_{16}+\left[1-\left(\frac{7.52a_s}{n_f\alpha\phi}\right)\right]y_{17}+y_{18}=0$$

--- (12)

By substituting Equation (8) into Equations (3), (10), (11) and (12), yields four equations with four main unknown y_1, y_2, y_3, and y_4. The resulting equations as shown below are nonlinear and best solved by Newton-Raphson iteration method (Yang, 2005).

$$y_1+y_2+y_3+y_4+c_5c_8\left(\frac{y_2}{y_1}\right)+c_5^2\left(\frac{y_2^2}{y_1^2}\right)+c_5^3c_9\left(\frac{y_2^3}{y_1^3}\right)+c_7y_1^{0.5}$$
$$+c_6\left(\frac{y_2}{y_1^{0.5}}\right)+\left(\frac{c_1}{c_5}\right)\left(\frac{y_1y_3}{y_2}\right)+\left(\frac{c_1c_2}{c_5^2}\right)\left(\frac{y_1^2y_3}{y_2^2}\right)+\left(\frac{c_1c_2c_3}{c_5^2}\right)\left(\frac{y_1^4y_3}{y_2^2}\right)$$
$$+c_5c_{11}\left(\frac{y_2y_4^{0.5}}{y_1}\right)+c_5^2c_{11}c_{12}\left(\frac{y_2^2y_4^{0.5}}{y_1^2}\right)+c_{13}y_4^{0.5}y_1^{1.5}$$
$$+c_5^{2.5}c_{11}c_{12}^{1.5}c_{14}^{0.5}\left(\frac{y_2^3y_4^{0.5}}{y_1^{2.5}}\right)+\left(\frac{c_1c_2c_4}{c_5^2}\right)\left(\frac{y_1^{2.5}y_3y_4^{0.5}}{y_2^2}\right)+c_{10}y_4^{0.5}-1=0$$

--- (13)

$$2y_1+2y_2-\left(\frac{n_f\beta+2p}{n_f\alpha}\right)y_3+c_7y_1^{0.5}+c_6\left(\frac{y_2}{y_1^{0.5}}\right)$$
$$-\left(\frac{n_f\beta+2p}{n_f\alpha}\right)\left(\frac{c_1}{c_5}\right)\left(\frac{y_1y_3}{y_2}\right)-\left(\frac{n_f\beta+2p}{n_f\alpha}\right)\left(\frac{c_1c_2}{c_5^2}\right)\left(\frac{y_1^2y_3}{y_2^2}\right)$$
$$+\left[4-\left(\frac{n_f\beta+2p}{n_f\alpha}\right)\right]\left(\frac{c_1c_2c_3}{c_5^2}\right)\left(\frac{y_1^4y_3}{y_2^2}\right)+3c_{13}y_4^{0.5}y_1^{1.5}$$
$$+c_5^{2.5}c_{11}c_{12}^{1.5}c_{14}^{0.5}\left(\frac{y_2^3y_4^{0.5}}{y_1^{2.5}}\right)$$
$$+\left[1-\left(\frac{n_f\beta+2p}{n_f\alpha}\right)\right]\left(\frac{c_1c_2c_4}{c_5^2}\right)\left(\frac{y_1^{2.5}y_3y_4^{0.5}}{y_2^2}\right)=0$$

--- (14)

$$y_2+\left[2-\left(\frac{2a_s}{n_f\alpha\phi}\right)\right]y_3+c_5c_8\left(\frac{y_2}{y_1}\right)+2c_5^2\left(\frac{y_2^2}{y_1^2}\right)+3c_5^3c_9\left(\frac{y_2^3}{y_1^3}\right)$$
$$+c_6\left(\frac{y_2}{y_1^{0.5}}\right)+\left(\frac{c_1}{c_5}\right)\left[1-\left(\frac{2a_s}{n_f\alpha\phi}\right)\right]\left(\frac{y_1y_3}{y_2}\right)$$
$$-\left(\frac{2a_s}{n_f\alpha\phi}\right)\left(\frac{c_1c_2}{c_5^2}\right)\left(\frac{y_1^2y_3}{y_2^2}\right)-\left(\frac{2a_s}{n_f\alpha\phi}\right)\left(\frac{c_1c_2c_3}{c_5^2}\right)\left(\frac{y_1^4y_3}{y_2^2}\right)$$
$$+c_5c_{11}\left(\frac{y_2y_4^{0.5}}{y_1}\right)+2c_5^2c_{11}c_{12}\left(\frac{y_2^2y_4^{0.5}}{y_1^2}\right)+3c_5^{2.5}c_{11}c_{12}^{1.5}c_{14}^{0.5}\left(\frac{y_2^3y_4^{0.5}}{y_1^{2.5}}\right)$$
$$-\left(\frac{2a_s}{n_f\alpha\phi}\right)\left(\frac{c_1c_2c_4}{c_5^2}\right)\left(\frac{y_1^{2.5}y_3y_4^{0.5}}{y_2^2}\right)=0$$

--- (15)

$$-\left(\frac{7.52a_s}{n_f\alpha\phi}\right)y_3+2y_4-\left(\frac{c_1}{c_5}\right)\left(\frac{7.52a_s}{n_f\alpha\phi}\right)\left(\frac{y_1y_3}{y_2}\right)$$
$$-\left(\frac{7.52a_s}{n_f\alpha\phi}\right)\left(\frac{c_1c_2}{c_5^2}\right)\left(\frac{y_1^2y_3}{y_2^2}\right)-\left(\frac{7.52a_s}{n_f\alpha\phi}\right)\left(\frac{c_1c_2c_3}{c_5^2}\right)\left(\frac{y_1^4y_3}{y_2^2}\right)$$
$$+c_5c_{11}\left(\frac{y_2y_4^{0.5}}{y_1}\right)+c_5^2c_{11}c_{12}\left(\frac{y_2^2y_4^{0.5}}{y_1^2}\right)+c_{13}y_4^{0.5}y_1^{1.5}$$
$$+c_5^{2.5}c_{11}c_{12}^{1.5}c_{14}^{0.5}\left(\frac{y_2^3y_4^{0.5}}{y_1^{2.5}}\right)$$
$$+\left[1-\left(\frac{7.52a_s}{n_f\alpha\phi}\right)\right]\left(\frac{c_1c_2c_4}{c_5^2}\right)\left(\frac{y_1^{2.5}y_3y_4^{0.5}}{y_2^2}\right)+c_{10}y_4^{0.5}=0$$

--- (16)

2.2. MATLAB Inputs

In this study, MATLAB codes for combustion modeling had been developed. The hydrocarbon fuel is to be specified in terms of C and H atoms and for hydrogen-diesel blends, the percentage of the blend need to be acknowledged. Apart from that, other inputs parameters that need to be provided into the MATLAB program are Combustion Temperature, T(K), Equivalence ratio,ϕ and Combustion Pressure, P(bar). In this paper, the percentage of hydrogen substitution and combustion pressure were fixed to constant values of 80% (by mass of diesel fuel) and 55 bar, respectively. Combustion temperatures are variable inputs that need to be specified at the beginning of the simulation. It has fixed values from 1600K, 2000K, 2500K, 3000K and 3500K. The output of the developed program is used to analyze the effects of combustion temperature on mole fractions of 18 products species with respect to specified equivalence ratios (phi,ϕ).

3. RESULT AND DISCUSSION

In this study, the effects of combustion temperature in emissions were analyzed based on the developed combustion model. Figure 1 shows the variation of mole fractions of H_2 with combustion temperature at constant pressure of 55 bar and 80% of hydrogen substitution. It can be noted during lean combustion (ϕ<1) there was no significant changes of H_2 when combustion temperature lower than 2500K but as the temperature increases, H_2 emission will also increase. When equivalence ratio, ϕ=1.2, mole fractions of H_2 starts to increase at the temperature of 3000K while at equivalence ratio, ϕ= 1.6 there was no significant effect of combustion temperature on H_2 emissions. In general, during rich combustion, the higher the temperature, the higher H_2 emissions in diesel engine.

Figure 2 shows that increase in combustion temperature decreases H_2O emission. There were no changes of H_2O emissions for all equivalence ratios until the combustion temperature reaches 3000K then it starts to decrease. The highest emission occurs when equivalence ratio equals to unity (stoichiometric combustion). The existence of H_2O at high temperature catalyzing the process of dissociation which forms additional H_2, this will be one of the reasons in the increase of H_2 emissions as discussed earlier.

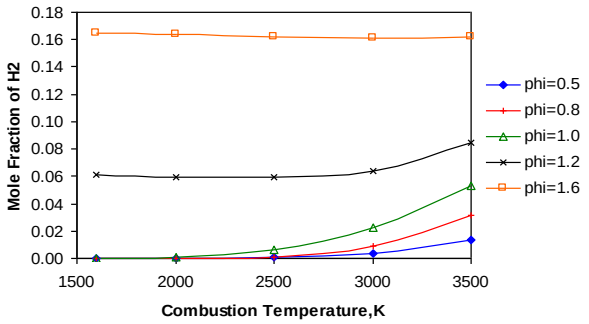

Figure 1: Mole of fraction of H_2 with variation of combustion temperature

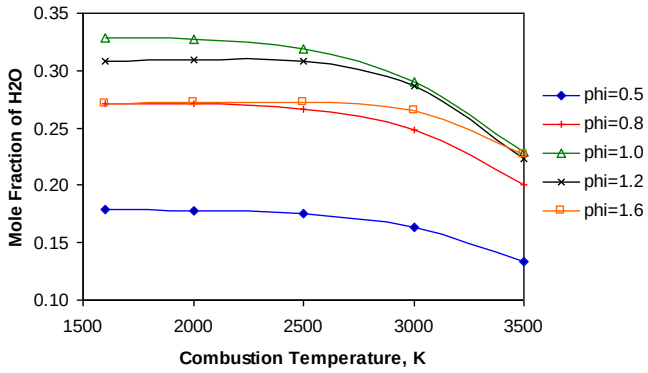

Figure 2: Mole of fraction of H_2O with variation of combustion temperature

The variation of mole fractions of CO_2 with combustion temperature is shown in Figure 3. It shows the maximum CO_2 concentration is reached at stoichiometric combustion (ϕ=1.0) whereas its concentrations are lower both in the lean and rich setting. CO_2 is one of the major species present at low combustion temperature (Schafer, 1995).

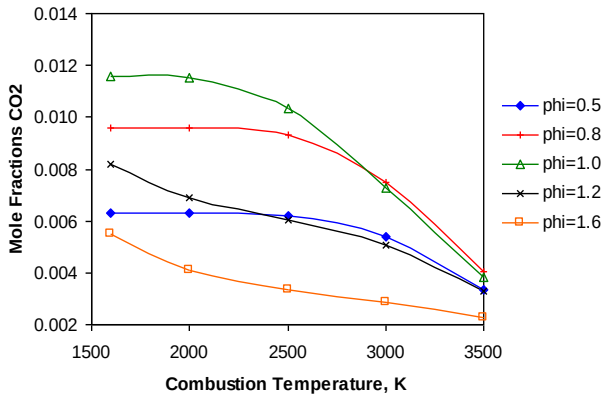

Figure 3: Mole of fraction of CO_2 with variation of combustion temperature

As the combustion temperature increases, mole fractions of CO_2 decreases as a result from dissociation process of CO_2 to form CO and O_2 species in significant amount (Glassman, 2008). It also shows decrease in amount when equivalence ratios are greater than unity. As an example for rich combustion (ϕ=1.2), mole fraction of CO_2 is reduced in between 15% to 35% as the combustion temperature increases from 1600K to 3500K.

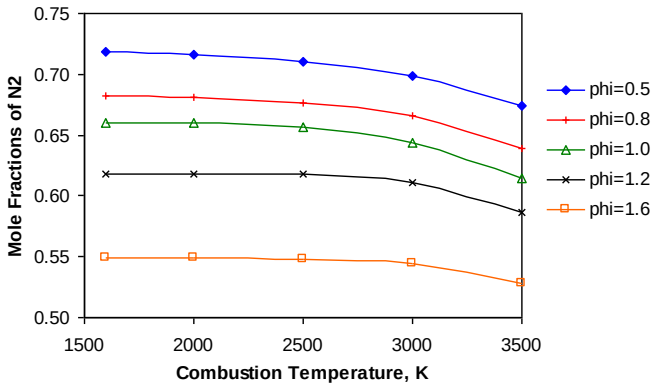

Figure 4: Mole of fraction of N_2 with variation of combustion temperature

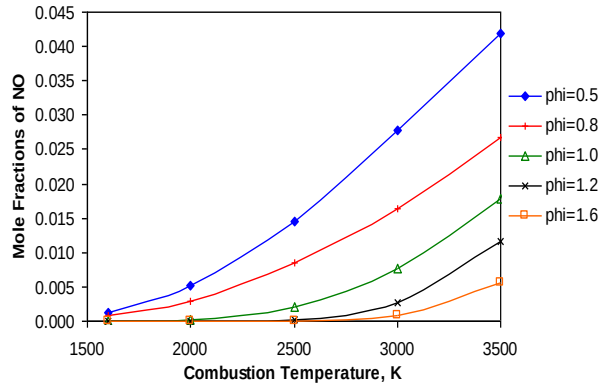

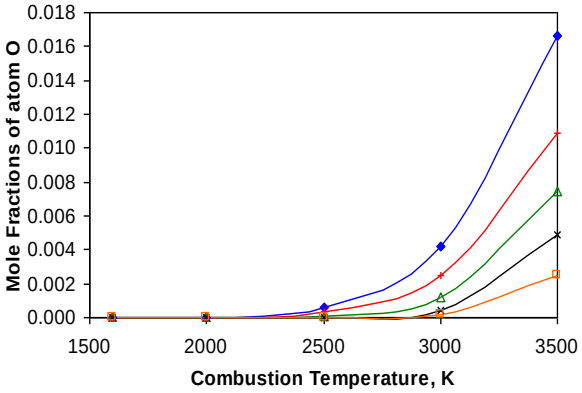

Figure 5: Mole of fractions of NO and atom O with variation of combustion temperature

Figure 4 shows the variations of mole fractions of N_2 with combustion temperature. It can be noted that as combustion temperature increases, mole fractions of N_2 decreases as the same trends shown thoughout all equivalence ratios. The highest emission of N_2 is shown during lean combustion at equivalence ratio,ϕ of 0.5. The richer the combustion, the lower N_2 emitted especially at high combustion temperature. Figure 5 shows the same trend of NO and atom O emissions versus combustion temperature. The increase of NO emissions occurs as the reaction of the extended Zeldovich mechanism is increased. With combustion temperature increases, mole fractions or concentration of NO and atom O emissions increases rapidly when temperatures are greater than 2500K. As shown, both are maximized with mixtures slightly lean since the increased temperatures favors NO formation. Generally, the formation of NO is highly dependent on in-cylinder temperatures, oxygen concentration and residence time for the reaction to take place (Andrea, 2004). It is proven that during lean combustion, the formation of NO and atom O increases with increasing temperature since excess air during combustion catalyzes the formation of both emissions, but there is little excess of oxygen in rich mixtures to dissociate and attach to nitrogen atoms to form nitric oxide. The interplay between these two effects results in maximum nitric oxides occurring in lean mixtures, where there is excess of oxygen atoms to react with the nitrogen atoms to form NO. Additionnally, the increase of NO emission in hydrogen-diesel dual fuel combustion is correlated to the faster burning rate of hydrogen (Naber, 1998).

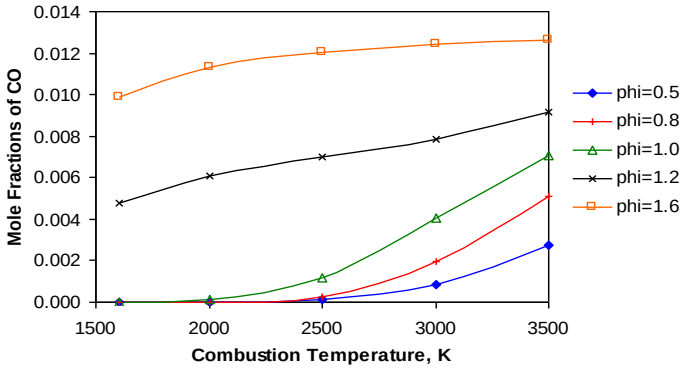

Figure 6: Mole of fraction of CO with variation of combustion temperature

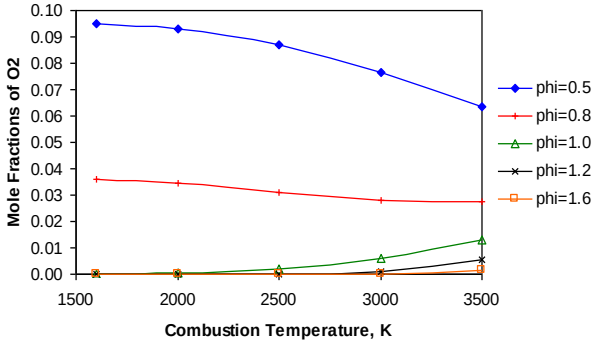

Figure 7: Mole of fraction of O_2 with variation of combustion temperature

Figure 6 shows that as the combustion temperature equivalence ratios increases, CO emission a increases. Mole fractions of CO showed a remarka high during rich combustion and temperatures gre than 2500K. CO is the minor species in the l combustion and as the mixture gets richer m fractions of CO increases due to incomplete combust of carbon. Futhermore, as the combustion temperat increases CO_2 dissociates to form CO and hence, m fraction of CO increases as temperature increa (William, 1985).

The variations of O_2 emission with combust temperature is shown in Figure 7. During lean combustion, mole fraction of O_2 decreases as combustion temperature increases. As equivalence ratio decreases, mole fraction of O_2 increases while the highest amount of O_2 occurs when the equvalence ratio equals to 0.5. During rich combustion, there was insignificant changes of O_2 emissions throughout all combustion temperature. The reason that, there is a greater amount of dissociation on the lean side is because the dissociation of one mole of CO_2 results in one mole of CO but only half mole of O_2. Thus the lean mixtures can accommodate more O_2 from dissociation than that of the rich mixtures (Chung, 2004).

Figure 8 shows the same trend of OH and NO_2 emissions versus combustion temperature. Mole fractions of both emissions increased as combustion temperature increases with the decrease in equivalence ratios. It can be seen that both emissions increases rapidly when combustion temperature greater than 2500K.

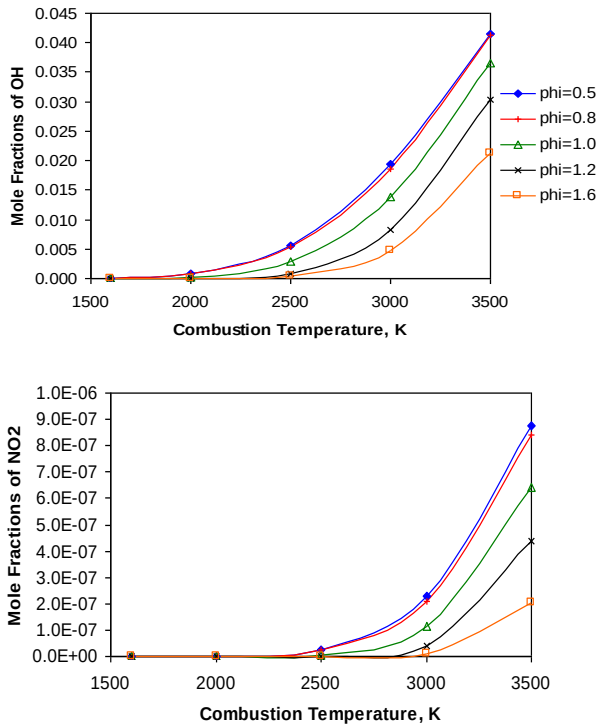

Figure 8: Mole of fractions of OH and NO_2 with variation of combustion temperature

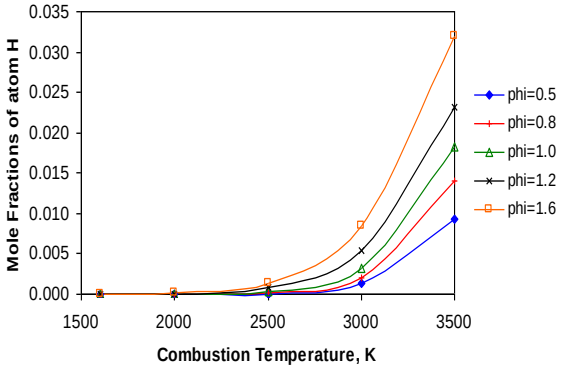

Figure 9: Mole of fraction of atom H with variation of combustion temperature

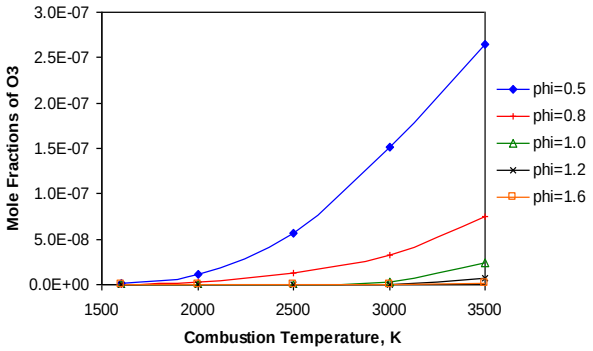

Figure 10: Mole of fraction of atom O_3 with variation of combustion temperature

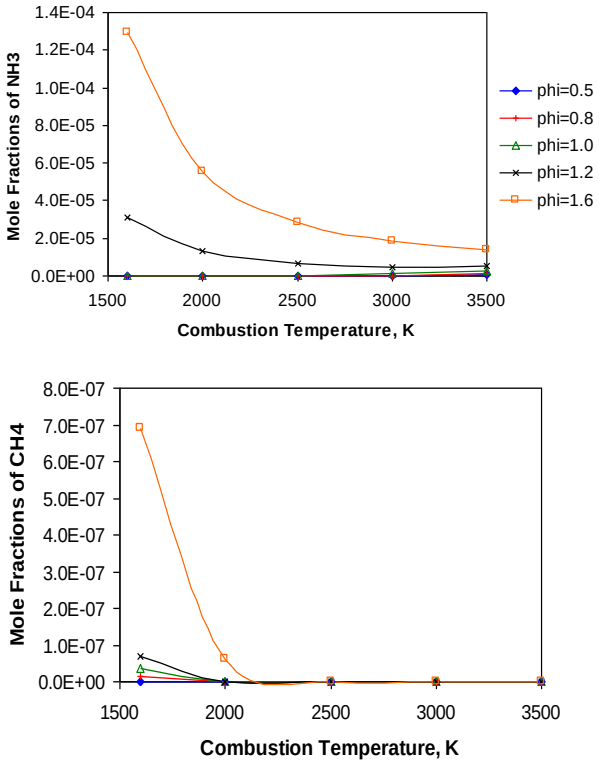

Figure 11: Mole of fractions of NH_3 and CH_4 with variation of combustion temperature

The variations of atom H with combustion temperature is shown in Figure 9. It can be seen during rich combustion, as equivalence ratio increases, mole fractions of atom H also increases and the highest amount of atom H occurs at temperature of 3500K in rich mixture. During lean and low temperature combustion, there was insignificant changes of atom H emissions throughout all equivalence ratios.

Figure 10 shows O_3 emissions versus combustion temperature. With combustion temperature increases, mole fractions of O_3 will also increase specifically when temperatures are greater than 2500K. It is maximized during lean combustion, as discussed earlier, increasing concentration of atom O promotes formation of O_3 after its reaction with O_2. This explains another possible reason about the reduction of O_2 concentration in excess air of lean mixture.

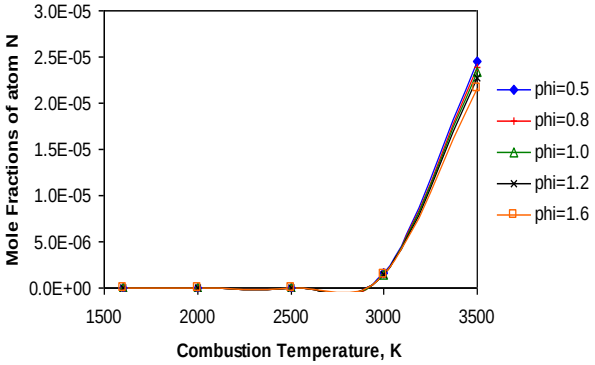

Figure 12: Mole of fraction of atom N with variation of combustion temperature

Figure 11 shows NH_3 and CH_4 emissions versus combustion temperature. With combustion temperature increases, mole fractions of NH_3 and CH_4 will decrease with respect to the increase in equivalence ratios. It can be seen that insignificant amount of both emissions during lean combustion regardless of any combustion temperature. Both emissions are classified as gaseous fuel, during lean combustion these fuels were burnt with excess air in the mixture (Pulkrabek, 2004). For rich combustion, late combustion of both emissions occurs when temperature greater than 2000K.

Figure 12 shows that as there were no changes of atom N formation in the exhaust species when combustion temperature less than 3000K, further increase in temperature increases formation of atom N for all equivalence ratios. Figure 13 below shows the change in mole fractions of HNO_3 for various combustion temperature and equivalence ratios. With the increase in temperature and equivalence ratio, HNO_3 emissions decreases until equivalence ratio equals to unity, further increase in equivalence ratio causes insignificant changes in HNO_3 emissions.

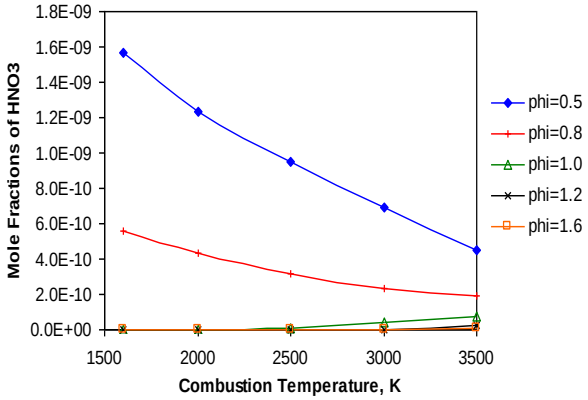

Figure 13: Mole of fraction of HNO_3 with variation of combustion temperature

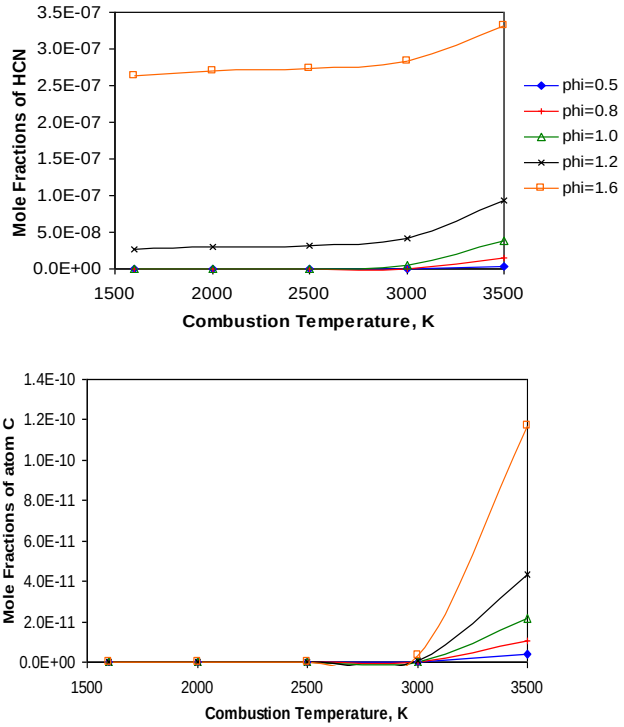

Figure 14: Mole of fractions of HCN and atom C with variation of combustion temperature

Figure 14 shows hydrocarbon emissions of HCN and atom carbon (C) versus combustion temperature. With combustion temperature increases, mole fractions of HCN and atom C will also increase specifically when temperatures are greater than 3000K. It also can be seen that there were insignificant changes of both emissions with respect to combustion temperature before 3000K. As the equivalence ratio increases greater than unity, the emissions of hydrocarbon also increases especially for HCN. This is due to insufficient air to react with the diesel fuel that remains in the exhaust. The molecules structure of the remaining diesel fuel will be altered by chemical reactions within the hot cylinder engine and hence increases the hydrocarbon emissions (Heywood, 1988).

4. CONCLUSIONS

The emissions characteristics of combustion in hydrogen-diesel dual fuel system was modeled by using Equilibrium Constant Method. From the above analysis and discussion, the conclusions made as following:

- Higher combustion temperature during rich combustion causes higher H_2, CO, HCN, atoms C and H emissions in hydrogen-diesel dual fuel system.
- Lower combustion temperature increases emissions of N_2, O_2 and HNO_3 during lean combustion.
- Lower combustion temperature has no significant effect on H_2O emission.
- Increase in combustion temperature leads to increase in mole fractions of NO, atom O, OH, NO_2 and O_3 with decreasing value of equivalence ratios.
- Combustion temperature less than 3000K shows insignificant changes in atom N emissions.
- Increase in combustion temperature decreases CO_2, NH_3 and CH_4 emissions for all equivalence ratios.

ACKNOWLEDGMENT

The work described in this paper is partly sponsored by Ministry of Science, Technology and Environment of Malaysia.

Nomenclature

NO	nitrogen oxide	ECM	Equilibrium Constant Method
CO	carbon monoxide	PHI(ϕ)	Equivalence Ratio
CO_2	carbon dioxide	H_2	hydrogen gas
HC	hydrocarbon	N	atom nitrogen
H	atom hydrogen	HNO_3	nitric acid
H_2O	water	O_3	tri-oxygen
O_2	oxygen	CH_4	methane gas
NH_3	ammonia	C	atom carbon
HCN	hydrogen cyanide	N_2	nitrogen gas
OH	hydroxide	NO_2	nitrogen dioxide

REFERENCES

Agrawal D.D, Gupta C.P, 1977. Computer program for constant pressure or constant volume combustions calculations in hydrocarbon–air systems, Trans.ASME, Engineering Power, 99, 246-255.

Andrea T.D, Henshaw P.F, Ting D.S.K, 2004. The addition of hydrogen to a gasoline-fueled SI engine, Hydrogen Energy, 29, 1541-1552.

Brenda J., Micheal C.M., Anshuman K., 2005. Hydrogen: the energy source for the 21st century, Technovation, 25, 569- 585.

Caton J.A, 2001. An investigation of cause of backfire and its control due to creviced volumes in hydrogen fueled engine, Trans. ASME, l.23, 204–210.

Chung K.L, 2006. Combustion Physics, first ed. Cambridge University Press, Cambridge, New York.

Ganesan V, 2003. Internal Combustion Engine,second ed. Tata McGraw-Hill, New Delhi.

Glassman I, Yetter, R.A, 2008. Combustion, fourth ed. Elsevier Inc., London

Heywood J.B., 1988. Internal Combustion Engine Fundamentals. Int. ed. McGraw-Hill Inc., New York

Karim G.A, 2003. Combustion in gas-fueled Compression ignition engines of the dual fuel type,Gas Turbine and Power,125, 827-836.

Lata D.B., Misra A., 2010. Theoretical and experimental investigationson the performance of dual fuel diesel engine with hydrogen and LPG as secondary fuels, 35, 11918-11931.

Ma J., Su Y., Zhou Y., Zhang Z., 2003. Simulation and prediction on the performance of a vehicle's hydrogen engine, Hydrogen Energy, l.28, 77-83.

Masood M., Ishrat M.M., 2008. Computer simulations of hydrogen–diesel dual fuel exhaust gas emissions with experimental verification, Fuel, 87, 1372–1378,

Naber J.D, Siebers D.L, 1998. Hydrogen combustion under diesel engine conditions, Hydrogen Energy, 23, 363-371.

Perini F., Paltrinieri F., Mattarelli E., 2010. A quasi-dimensional combustion model for performance and emissions of SI engines running on hydrogen-methane blends, Hydrogen Energy, 35, 4687-4701.

Pulkrabek W.W., 2004. Engineering Fundamentals of The Internal Combustion Engine. Second ed. PearsonPrentice-Hall, New Jersey.

Roy M.M., Tomita E., Kawahara N., Harada Y.,Sakane A., 2009. Performance and emission comparison of a supercharged dual-fuel engine fueled by producer gases with varying hydrogen content, Hydrogen Energy, 34, 7811-7822.

Saravanan N., Nagarajan G., Narayanasamy S., 2008. An experimental investigation on DI diesel engine with hydrogen fuel, Renewable, Energy, 1.33, 415-421.

Schafer F, Basshuysen R.V, 1995. Reduced Emissions and Fuel Consumption in Automobile, first ed. Springer- Verlag Wien, New York, 1995.

Stephen R.T, 2000. An Introduction to Combustion: Concepts and Applications, second ed. McGraw-Hill,New York.

Stull D.R., Prophet H.,1971. JANAF Thermochemical Tables, National Bureau of Standards Publication NSRDS- NBS37, Washington.

Verhelst S., Sierens R., 2007. A quasi-dimensional model for the power cycle of a hydrogen- fuelled ICE, Hydrogen Energy 32, 3545 – 3554.

Wang Y., Zhang X., Li C., Wu J., 2010. Experimental and modeling study of performance and emissions of SI engine fueled by natural gas- hydrogen mixtures, Hydrogen Energy, 35, 2680-2683.

Williams F.A, 1985. Combustion Theory: The Fundamental Theory of Chemically Reacting Flow Systems, second ed. The Benjamin/Cummings Publishing Company, Inc., California, USA.

Xing-hua L, Fu-shui L, Lei Z, Bai-gang S,Harold J.S, 2008. Backfire prediction in a manifold injection hydrogen internal combustion engine, Hydrogen Energy, 33, 3847- 3855.

Yang W.Y, Cao W., Chung T.S, Morris J, 2005. Applied Numerical Method Using Matlab, second ed. John Wiley and Sons, New Jersey.